

# Synthesis and Luminescence Properties of (Y, Gd) (P, V)O<sub>4</sub>:Eu<sup>3+</sup>, Bi<sup>3+</sup> Red Nano-phosphors with Enhanced Photoluminescence by Bi<sup>3+</sup>, Gd<sup>3+</sup> Doping

Yong Pu<sup>1</sup>, Ke Tang<sup>2,#</sup>, Da-Chuan Zhu<sup>1,\*</sup>, Tao Han<sup>1,3</sup>, Cong Zhao<sup>1</sup>, Ling-Ling Peng<sup>3</sup>

(Received 16 Jan 2013; accepted 13 May 2013; published online 26 May 2013)

**Abstract:** A series of (Y<sub>1-y</sub>, Gd<sub>y</sub>)<sub>0.95-x</sub>(P<sub>y</sub>, V<sub>1-y</sub>)O<sub>4</sub>:0.05Eu<sup>3+</sup>, xBi<sup>3+</sup> phosphors have been successfully prepared by a subsection method. The crystal structure, surface morphology and luminescence properties were investigated. It was found that the sintered samples crystallized in a tetragonal crystal system with space group I<sub>41/amd</sub> ( $a = b = 0.7119$  nm,  $c = 0.6290$  nm). The products presented rod-like morphology with length of 100-150 nm and width of 50-100 nm. A maximum peak at 619 nm (<sup>5</sup>D<sub>0</sub> → <sup>7</sup>F<sub>2</sub>) was observed in emission spectrum of the phosphors. It was also found that co-doping of Bi<sup>3+</sup>, P<sup>5+</sup> and Gd<sup>3+</sup> ions into YVO<sub>4</sub>:Eu<sup>3+</sup> can not only made the right edge of the excitation band shift to the long-wavelength region, but also increased the emission intensity at 619 nm sharply and decreased the lifetime of fluorescence decay. These results may expand the application scope of the phosphors.

**Keywords:** (Y, Gd)(P, V)O<sub>4</sub>:Eu<sup>3+</sup>, Bi<sup>3+</sup>; Rod-like; Red phosphors; Photoluminescence; Doping

**Citation:** Yong Pu, Ke Tang, Da-Chuan Zhu, Tao Han, Cong Zhao and Ling-Ling Peng, "Synthesis and Luminescence Properties of (Y, Gd)(P, V)O<sub>4</sub>:Eu<sup>3+</sup>, Bi<sup>3+</sup> Red Nano-phosphors with Enhanced Photoluminescence by Bi<sup>3+</sup>, Gd<sup>3+</sup> Doping", Nano-Micro Lett. 5(2), 117-123 (2013). <http://dx.doi.org/10.5101/nml.v5i2.p117-123>

## Introduction

Over past decades, many efforts have been made to study the rare-earth doped luminescence materials, which have been largely applied in fields of illuminations and displays, such as fluorescent lamps, cathode-ray tubes, field emission displays, plasma display panels, electro-optical polarizers and white light-emitting diodes [1-7]. Yttrium vanadate (YVO<sub>4</sub>) has been proved one of the best candidates for doping into rare earth ions [8] since it provides a suitable Y<sup>3+</sup> site where trivalent rare-earth ions can be replaced without additional charge compensation. In particular, as a typical red-emitting phosphor, europium doped YVO<sub>4</sub>

has been explored in many fields [8-11]. Recent years, much attention has been focused on the nanoscale phosphors. It was found that the higher packing density and better paste rheology of smaller-sized phosphors particles led to higher screen resolution and lower screen load [12-16]. Especially, Eu<sup>3+</sup> doped nanoscaled YVO<sub>4</sub> phosphor has attracted a great deal of attention. Nowadays, a number of methods, such as single crystal growth techniques, the solution combustion process, hydrolyzed colloid reaction (HCR), solution-based sol-gel process and hydrothermal reaction have been used to synthesize the YVO<sub>4</sub>:Eu<sup>3+</sup> nanophosphors. However, due to lower crystallinity and higher surface defect density, most products have lower luminescent intensity compared with their bulk powders. For exam-

<sup>1</sup>College of Material Science and Engineering, Sichuan University, Sichuan Chengdu, 610065, China

<sup>2</sup>College of Information Engineering, Chengdu University of Technology, Sichuan Chengdu, 610059, China

<sup>3</sup>Chongqing Key Laboratory of Micro/Nano Materials Engineering and Technology, Chongqing, 402168, China

#This author contributed equally as the co-first author

\*Corresponding author. E-mail: zdc89@163.com, puyong456@sina.com

ple, compared with commercial PDP red phosphor ( $\text{Y, Gd}\text{BO}_3\text{:Eu}^{3+}$ ,  $\text{YVO}_4\text{:Eu}^{3+}$  nanoparticles have higher color purity but lower luminescent intensity, especially when the particle size decreased into nanosized scale [15].

Many efforts have been made to improve luminescence properties of  $\text{YVO}_4\text{:Eu}^{3+}$  nanophosphors [17-21]. For example, sensitizer co-doping has been proved to be an efficient way to increase the luminescent efficiency. Till now, many researches are focused on one kind of ions doped into  $\text{YVO}_4\text{:Eu}^{3+}$  nanophosphors. It is relatively less reports on multi-ions co-doping. It was found that high concentration doping of  $\text{Gd}^{3+}$  and  $\text{P}^{5+}$  into  $\text{YVO}_4\text{:Eu}^{3+}$  would increase the photoluminescence intensity [3,19]. And  $\text{Bi}^{3+}$  ion can be used as a sensitizer to strengthen and broaden the ultraviolet-vacuum ultraviolet (UV-VUV) excitation bands [10]. In this paper, three kinds of ions ( $\text{Bi}^{3+}$ ,  $\text{P}^{5+}$  and  $\text{Gd}^{3+}$ ) were co-doped into  $\text{YVO}_4\text{:Eu}^{3+}$  to improve the photoluminescence properties by using a subsection method.

## Experimental

### Materials and reagents

The materials and reagents used in the experiment were  $\text{Y}_2\text{O}_3$  (99.99% purity),  $\text{Gd}_2\text{O}_3$  (99.99% purity),  $\text{Eu}_2\text{O}_3$  (99.99% purity),  $\text{Bi}(\text{NO}_3)_3 \cdot 5\text{H}_2\text{O}$  (A.R.),  $\text{NH}_4\text{VO}_3$  (A.R.),  $(\text{NH}_4)_2\text{HPO}_4$  (A.R.),  $\text{HNO}_3$  (A.R.), Polyethylene glycol (PEG, molecular weight=20000, A.R.), Anhydrous ethanol (A.R.),  $\text{NH}_3 \cdot \text{H}_2\text{O}$  (A.R.), Citric acid (A.R.) and enough distilled water.

### Synthesis of $(\text{Y, Gd})(\text{P, V})\text{O}_4\text{:Eu}^{3+}$ , $\text{Bi}^{3+}$ samples

All samples were prepared by a two-step subsection method. The  $\text{YVO}_4\text{:Eu}^{3+}$ ,  $\text{Bi}^{3+}$  crystal seeds were prepared by a solvothermal method and  $\text{Gd}^{3+}$ ,  $\text{P}^{5+}$  were doped into  $\text{YVO}_4\text{:Eu}^{3+}$ ,  $\text{Bi}^{3+}$  by a sol-gel process. In a typical solvothermal synthesis process,  $(\text{Y}_{0.5}, \text{Gd}_{0.5})_{0.9}(\text{P}_{0.5}, \text{V}_{0.5})\text{O}_4\text{:0.05Eu}^{3+}, 0.05\text{Bi}^{3+}$  was successfully prepared through the following procedures. Firstly, proper quantity of  $\text{Y}_2\text{O}_3$  and  $\text{Eu}_2\text{O}_3$  were dissolved in excess diluted nitric acid to form a mixture. Then, proper quantity of  $\text{Bi}(\text{NO}_3)_3 \cdot 5\text{H}_2\text{O}$  and  $\text{NH}_4\text{VO}_3$  (molar ratio of  $\text{Y:Eu:Bi:V} = 0.90:0.05:0.05:1$ ), 50 ml anhydrous ethanol and distilled water ( $\text{E:W} = 1:1$ ) were mixed and added into the above mixture under ultrasonic mixing for 0.5 h to form a total solution. The initial pH value of the solution was adjusted to 7 using  $\text{NH}_3 \cdot \text{H}_2\text{O}$ . After that, the solution was transferred into a 100 ml stainless steel Teflon-lined autoclave and heated at  $200^\circ\text{C}$  for 12 h. After filtered and washed with distilled water by ethanol several times, the product was dried and white  $\text{YVO}_4\text{:Eu}^{3+}$  nanoparticles was

obtained.

In the sol-gel process, proper quantity of  $\text{Gd}_2\text{O}_3$ ,  $\text{Eu}_2\text{O}_3$  and  $(\text{NH}_4)_2\text{HPO}_4$  ( $\text{Gd:Eu:P} = 0.95:0.05:1$ ) were dissolved in excess diluted nitric acid and evaporated to dryness. The mixture was then dissolved in a 50 ml mixed solution of anhydrous ethanol and distilled water ( $\text{E:W} = 1:1$ ). Proper quantity of citric acid was added as a chelating agent for the metal ions under magnetic stirring (the molar ratio of metal ions to citric acid was 1:2). The proper quantity of polyethylene glycol (molecular weight = 10000, A.R.) was added as a cross-linking agent. Afterwards, a certain quantity of  $\text{YVO}_4\text{:Eu}^{3+}$  nanoparticles, which obtained in the solvothermal method process, were added under stirring. The pH value of the solution was adjusted to 2 by using  $\text{NH}_3 \cdot \text{H}_2\text{O}$  and the solution was stirred at  $60^\circ\text{C}$  for 1 h to form a gel. The gel was dried in an oven at  $100^\circ\text{C}$  and ground in an agate mortar for 10-30 min. The porous dried gel was then sintered at  $1000^\circ\text{C}$  for 2 h.

## Characterization

The structure of the products was analyzed by using a SHIMADZU polycrystalline XRD (Xpert PRD MPD) with  $\text{Cu-K}\alpha$  radiation (40 kV, 40 mA,  $\text{K}\alpha = 0.15418$  nm). The surface morphology was observed by a JEOL-JSM5900 and a Quanta 450 scanning electron microscopy (SEM). The excitation spectra, emission spectra and decay curves were recorded on a HITACHI F-7000 fluorescence spectrophotometer. All the measurements were done at room temperature.

## Results and discussion

Figure 1 shows the collected XRD patterns of (a)  $\text{Y}_{0.95}\text{VO}_4\text{:0.05Eu}^{3+}$  crystal seeds, (b)  $\text{Y}_{0.9}\text{VO}_4\text{:0.05Eu}^{3+}, 0.05\text{Bi}^{3+}$  crystal seeds, (c) the precursor prepared in the sol-gel process and (d) the final products  $(\text{Y}_{0.5}, \text{Gd}_{0.5})_{0.9}(\text{P}_{0.5}, \text{V}_{0.5})\text{O}_4\text{:0.05Eu}^{3+}, 0.05\text{Bi}^{3+}$  crystals sintered at  $1000^\circ\text{C}$  for 2 h. In order to explore the phase structure, the diffraction peaks of the samples are indexed on the basis of the single crystal  $\text{YVO}_4$  (JCPDS No. 17-0341) in a tetragonal crystal system with space group  $\text{I}_{41}/\text{amd}$  and  $\text{GdPO}_4$  (JCPDS No. 32-0386) in a monoclinic system with space group  $\text{P}_{21}/n$ . All XRD peaks in Fig. 1(a) are in good agreement with the values of standard  $\text{YVO}_4$  (JCPDS No. 17-0341). Since  $\text{Eu}^{3+}$  and  $\text{Y}^{3+}$  ions have the same valence and similar atomic radius, the doped  $\text{Eu}^{3+}$  has little effect on the structure of  $\text{YVO}_4$ . Compared with Fig. 1(a), Fig. 1(b) indicates a pure phase of  $\text{Y}_{0.9}\text{VO}_4\text{:0.05Eu}^{3+}, 0.05\text{Bi}^{3+}$  without obvious impurities. It can be also observed that  $\text{Bi}^{3+}$  doping will strengthen the peak intensity. In Fig. 1(c),

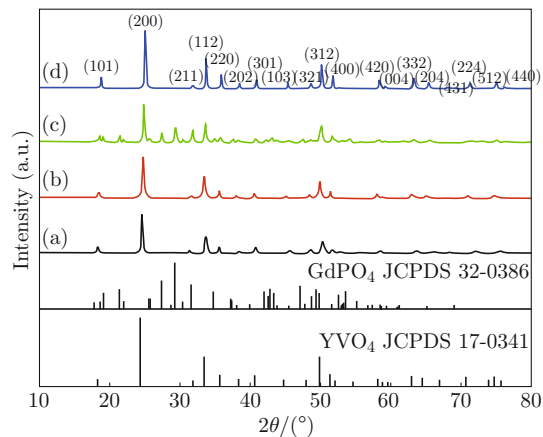


Fig. 1 XRD patterns of (a)  $\text{Y}_{0.95}\text{VO}_4: 0.05\text{Eu}^{3+}$ ; (b)  $\text{Y}_{0.9}\text{VO}_4: 0.05\text{Eu}^{3+}, 0.05\text{Bi}^{3+}$ ; (c) precursor prepared in the sol-gel process; (d)  $(\text{Y}_{0.5}, \text{Gd}_{0.5})_{0.9}(\text{P}_{0.5}, \text{V}_{0.5})\text{O}_4: 0.05\text{Eu}^{3+}, 0.05\text{Bi}^{3+}$  particles annealed at  $1000^\circ\text{C}$  for 2 h.

a mixture containing  $\text{YVO}_4$  and  $\text{GdPO}_4$  was found. However, the peaks for  $\text{GdPO}_4$  phase were not observed in final product (see Fig. 1(d)). The samples still keep a tetragonal phase with space group  $I_{41}/amd$  ( $a = b = 0.7119 \text{ nm}$ ,  $c = 0.6290 \text{ nm}$ ), which indicates  $\text{Gd}^{3+}$  and  $\text{P}^{5+}$  were doped in the sample after sintered

at  $1000^\circ\text{C}$  for 2 h. In addition, a systematic shifting of diffraction angle  $2\theta$  towards larger angle directions was observed, which is due to the different radius of the host ions and the doping ions. Since the radius difference between  $\text{V}^{5+}$  and  $\text{P}^{5+}$  is bigger than that between  $\text{Y}^{3+}$  and  $\text{Gd}^{3+}$ , the cell volumes decreased with increasing the same content rates of  $\text{Gd}^{3+}$  ( $\text{Eu}^{3+}$ ,  $\text{Bi}^{3+}$ ) and  $\text{P}^{5+}$ . As a result, the diffraction peaks shifted to the larger angle gradually.

Figure 2 shows SEM images of several representative samples. One can see that the merchant phosphors in Fig. 2(a) are composed of large grains with average size about  $1 \mu\text{m}$ . However, the seeds shown in Fig. 2(b) have spherical or approximately spherical morphology with about  $50 \text{ nm}$  in size, and the as-prepared particles (see Fig. 2((c),(d)) are short rod-like with average size about  $100 \text{ nm}$  length and  $50 \text{ nm}$  width. From Fig. 2(c,d), it was also found that the particles obtained by the solvothermal method are more uniform than those by the hydrothermal method. Figure 3 shows SEM images of  $\text{Y}_{1-x}, \text{Gd}_x)_{0.9}(\text{P}_x, \text{V}_{1-x})\text{O}_4: 0.05\text{Eu}^{3+}, 0.05\text{Bi}^{3+}$  with different doping content. One can see that the particle sizes increase gradually with the quantity of  $\text{Gd}^{3+}$  and  $\text{P}^{5+}$  doping. When doping quantity  $x$  is 0.5, the

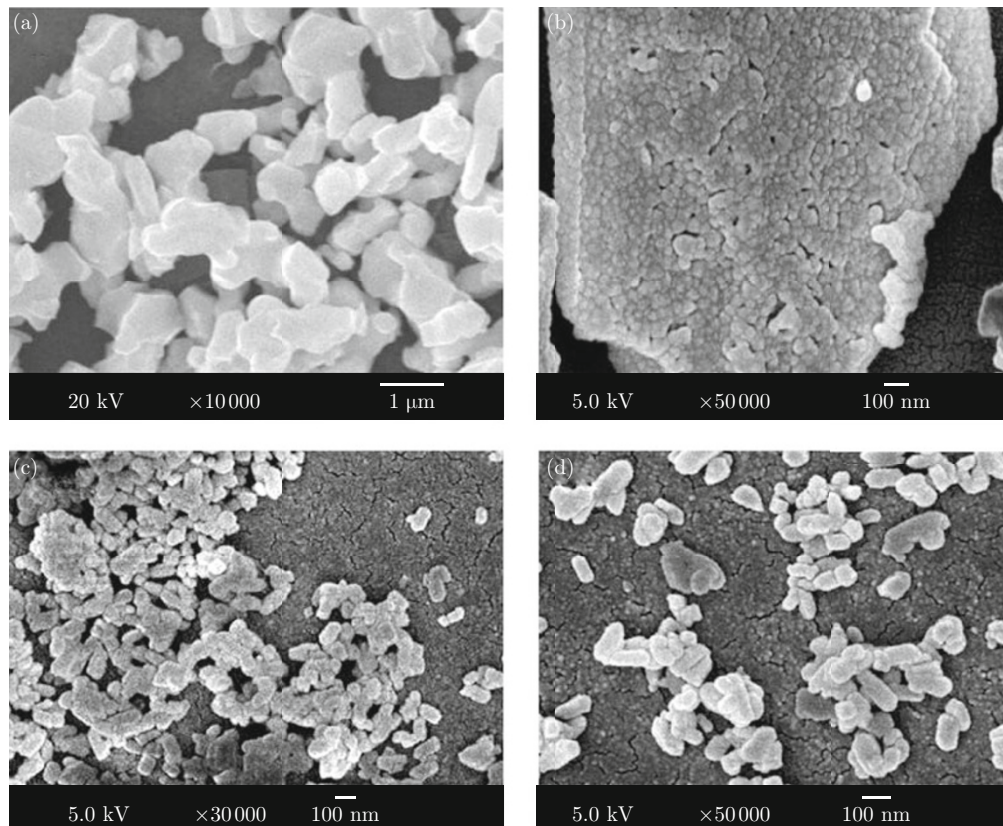


Fig. 2 SEM images of (a) the  $\text{Y}(\text{P}, \text{V})\text{O}_4: \text{Eu}^{3+}$  merchant phosphors prepared by HT method; (b)  $\text{YVO}_4: \text{Eu}^{3+}, \text{Bi}^{3+}$  crystal seeds; (c, d) the final  $(\text{Y}_{0.5}, \text{Gd}_{0.5})_{0.9}(\text{P}_{0.5}, \text{V}_{0.5})\text{O}_4: 0.05\text{Eu}^{3+}, 0.05\text{Bi}^{3+}$  samples prepared by the hydrothermal and solvothermal method, respectively.

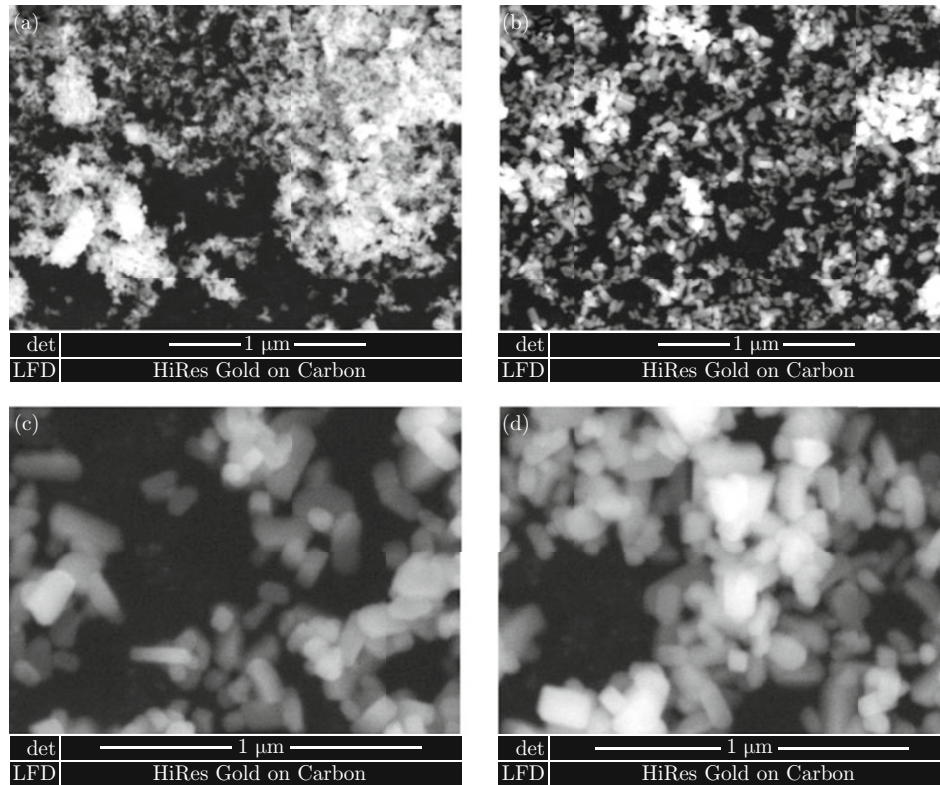


Fig. 3 SEM images of  $(Y_{1-x}, Gd_x)_{0.9} (P_x, V_{1-x}) O_4:0.05Eu^{3+}, 0.05Bi^{3+}$  crystals with (a)  $x = 0$ ; (b)  $x = 0.25$ ; (c)  $x = 0.5$ ; (d)  $x = 0.75$ .

particles present normal rod-like morphology and the particle size increases obviously. When doping quantity  $x$  is up to 0.75, the sample consists of irregular particles. These results indicate that co-doping  $Gd^{3+}$  and  $P^{5+}$  will increase the particle size and change the particle morphology obviously. This can be understood that  $YVO_4$  particles prepared by the solvothermal method played a role as template to control the shape of the final products due to the template-induced effect of the seed. During the calcine processes, the  $P^{5+}$  and  $Gd^{3+}$  ions were diffused into the  $YVO_4$  particles readily. It will weaken the limit effect of the seeds through increase the concentration of  $P^{5+}$  and  $Gd^{3+}$  ions continuously so that the phosphor particles approach to natural growth. Moreover, the rare earth orthophosphates generally have hexagonal or tetragonal structure and tend to form a wire-like or rod-like morphology [22].

Figure 4 shows the excitation spectra of (a)  $Y_{0.95}VO_4:0.05Eu^{3+}$ , (b)  $Y_{0.9}VO_4:0.05Eu^{3+}, 0.05Bi^{3+}$ , (c)  $Y_{0.9}(P_{0.5}, V_{0.5})O_4:0.05Eu^{3+}, 0.05Bi^{3+}$  and (d)  $(Y_{0.5}, Gd_{0.5})_{0.9}(P_{0.5}, V_{0.5})O_4:0.05Eu^{3+}, 0.05Bi^{3+}$  phosphors. The excitation spectra were measured in the range of 200-500 nm by monitoring the emission of  $Eu^{3+}$  at 619 nm ( ${}^5D_0 \rightarrow {}^7F_2$ ). As shown in Fig. 4(a), the excitation spectrum of  $Y_{0.95}VO_4:0.05Eu^{3+}$  consists of a broad band (210-350 nm) which is owing to the overlap of two peaked at about 275 and 325 nm. The short-wavelength excitation is due to the

charge-transfer processes involving the Y-O components, while the long-wavelength excitation is due to the V-O components of the matrix [15]. When  $Bi^{3+}$  is doped into  $Y_{0.95}VO_4:0.05Eu^{3+}$  particles, the intensity of the charge transfer (CT) bands (Eu-O and V-O interactions) increased and the right edge of the band shifted to near 400 nm (Fig. 4(b)), which ascribed to the intense absorption of  $Bi^{3+}$  compounds in the band of 250-400 nm. Related reports show that the absorption energy of  $Bi^{3+}$  could transfer to  $Eu^{3+}$ , which can

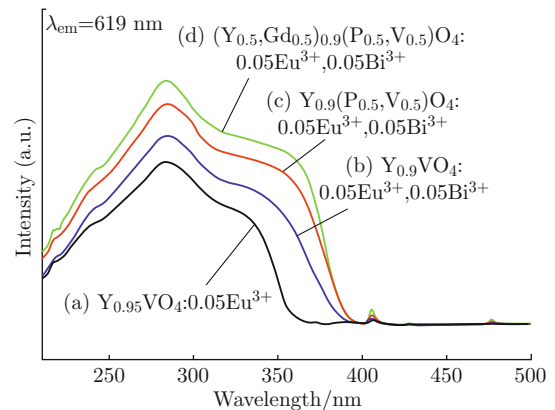


Fig. 4 The excitation spectra of (a)  $Y_{0.95}VO_4:0.05Eu^{3+}$ ; (b)  $Y_{0.9}VO_4:0.05Eu^{3+}, 0.05Bi^{3+}$ ; (c)  $Y_{0.9}(P_{0.5}, V_{0.5})O_4:0.05Eu^{3+}, 0.05Bi^{3+}$ ; and (d)  $(Y_{0.5}, Gd_{0.5})_{0.9}(P_{0.5}, V_{0.5})O_4:0.05Eu^{3+}, 0.05Bi^{3+}$  phosphors ( $\lambda_{em} = 619$  nm).

sensitize and enhance the intensity of  $\text{Eu}^{3+}$  [18]. When  $\text{P}^{5+}$  is doped into the  $\text{Y}_{0.9}\text{VO}_4:0.05\text{Eu}^{3+},0.05\text{Bi}^{3+}$  particles, the intensity of the excitation spectra will increase (Fig. 4(c)), especially the intensity of the band 320 nm-375 nm will enhance obviously. It may be resulted that doping of  $\text{P}^{5+}$  can enhance the CT band of  $\text{Bi}^{3+}-\text{O}^{2-}$  efficiently [19]. Furthermore, the intensity of the excitation spectra increased when  $\text{Gd}^{3+}$  is doped into the sample (Fig. 4(d)). This is because co-doping  $\text{Gd}^{3+}$  can produce more efficient excitation of  $\text{Eu}^{3+}$  in UV region [15].

Figure 5(a) shows emission spectra of  $\text{Y}_{0.95}\text{VO}_4:0.05\text{Eu}^{3+}$ ;  $\text{Y}_{0.9}\text{VO}_4:0.05\text{Eu}^{3+}, 0.05\text{Bi}^{3+}$ ;  $\text{Y}_{0.9}(\text{P}_{0.5}, \text{V}_{0.5})\text{O}_4:0.05\text{Eu}^{3+}, 0.05\text{Bi}^{3+}$  and  $(\text{Y}_{0.5}, \text{Gd}_{0.5})_{0.9}(\text{P}_{0.5}, \text{V}_{0.5})\text{O}_4:0.05\text{Eu}^{3+}, 0.05\text{Bi}^{3+}$  phosphors.

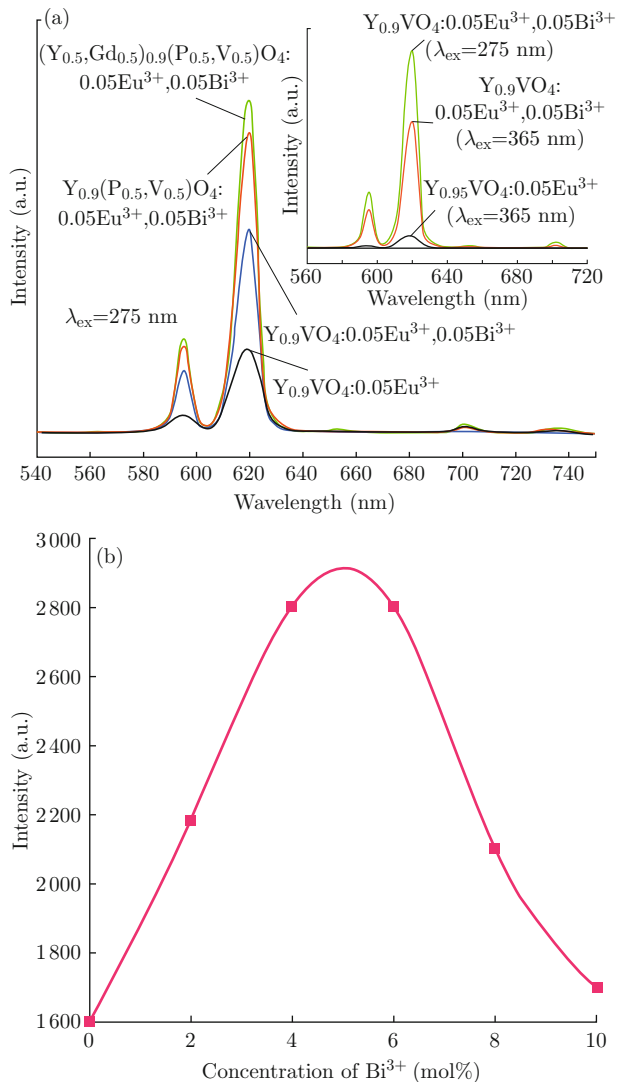


Fig. 5 (a) The emission spectra of  $\text{Y}_{0.95}\text{VO}_4:0.05\text{Eu}^{3+}$ ,  $\text{Y}_{0.9}\text{VO}_4:0.05\text{Eu}^{3+}, 0.05\text{Bi}^{3+}$ ,  $\text{Y}_{0.9}(\text{P}_{0.5}, \text{V}_{0.5})\text{O}_4:0.05\text{Eu}^{3+}, 0.05\text{Bi}^{3+}$  and  $(\text{Y}_{0.5}, \text{Gd}_{0.5})_{0.9}(\text{P}_{0.5}, \text{V}_{0.5})\text{O}_4:0.05\text{Eu}^{3+}, 0.05\text{Bi}^{3+}$  phosphors. The inset shows the emission spectra under 365 nm excitation. (b) The influence of  $\text{Bi}^{3+}$  concentration on relative emission intensity of  $(\text{Y}_{0.5}, \text{Gd}_{0.5})_{0.95-x}(\text{P}_{0.5}, \text{V}_{0.5})\text{O}_4:0.05\text{Eu}^{3+}, x\text{Bi}^{3+}$  at 619 nm ( $\lambda_{\text{ex}}=275$  nm).

$\text{Y}_{0.5})\text{O}_4:0.05\text{Eu}^{3+},0.05\text{Bi}^{3+}$  phosphors. For all the phosphors, two typical emission peaks of  $\text{Eu}^{3+}$  activators are located mainly in the red region (594 nm and 619 nm), which is due to the  ${}^5\text{D}_0 \rightarrow {}^7\text{F}_1$  and  ${}^5\text{D}_0 \rightarrow {}^7\text{F}_2$  transitions when excited under 275 nm. The emission peak near 700 nm is associated with the  ${}^5\text{D}_0 \rightarrow {}^7\text{F}_4$  transition. The strongest emission peak is at 619 nm indicating the final products have fine color purity. It can be obviously seen from Fig. 5(a) that the emission intensity at 619 nm under 275 nm excitation increased after  $\text{Bi}^{3+}$  doping into  $\text{YVO}_4:\text{Eu}^{3+}$ . It is also obvious that co-doping of  $\text{P}^{5+}$  and  $\text{Gd}^{3+}$  can enhance the emission intensity. This is because the incorporation of  $\text{P}^{5+}$  and  $\text{Gd}^{3+}$  into the  $\text{YVO}_4:\text{Eu}^{3+}$ ,  $\text{Bi}^{3+}$  lattice will increase the absorption of excitation energy and produce more efficient excitation of  $\text{Eu}^{3+}$ , thus enhancing the PL characteristics. The emission spectrum of  $\text{Y}_{0.9}\text{VO}_4:0.05\text{Eu}^{3+}, 0.05\text{Bi}^{3+}$  excited under 365 nm is shown in the inset of Fig. 5(a). One can find that the emission intensity of  ${}^5\text{D}_0 \rightarrow {}^7\text{F}_2$  electric dipole transition of  $\text{Eu}^{3+}$  at 619 nm under 365 nm excitation, which has about two-thirds intensity of that under 275 nm excitation, increases sharply with the doping of  $\text{Bi}^{3+}$  ions. It indicates that  $\text{Bi}^{3+}$  doping can obviously enhance the emission intensity at 619 nm when excited under 365 nm. Figure 5(b) shows the influence of  $\text{Bi}^{3+}$  concentration on the relative emission intensity of  $(\text{Y}_{0.5}, \text{Gd}_{0.5})_{0.95-x}(\text{P}_{0.5}, \text{V}_{0.5})\text{O}_4:0.05\text{Eu}^{3+}, x\text{Bi}^{3+}$  at 619 nm under 275 nm excitation. The curve shows that with increase of  $\text{Bi}^{3+}$  concentration, the emission intensity increased. As  $\text{Bi}^{3+}$  concentration is more than 5 mol%, the luminous intensity decreases gradually. The sensitization of  $\text{Bi}^{3+}$  to  $\text{Eu}^{3+}$  depends on the concentration of  $\text{Bi}^{3+}$ , and the most suitable concentration of  $\text{Bi}^{3+}$  is 5 mol%.

Figure 6 shows a comparison of the room-temperature luminescence decay curves of the  ${}^5\text{D}_0 \rightarrow {}^7\text{F}_2$  transition of  $\text{Eu}^{3+}$  between  $\text{Y}_{0.95}(\text{P}_{0.5}, \text{V}_{0.5})\text{O}_4:0.05\text{Eu}^{3+}$ ,  $(\text{Y}_{0.5}, \text{Gd}_{0.5})_{0.95}(\text{P}_{0.5}, \text{V}_{0.5})\text{O}_4:0.05\text{Eu}^{3+}$  and  $(\text{Y}_{0.5}, \text{Gd}_{0.5})_{0.9}(\text{P}_{0.5}, \text{V}_{0.5})\text{O}_4:0.05\text{Eu}^{3+}, 0.05\text{Bi}^{3+}$  under 275 nm excitation. The decay kinetics behavior depends on the number of different luminescent centers, defects, energy transfer and impurities in the host [23]. It is possible to explore the influence of co-doped elements on the decay dynamics of the samples. It can be clearly seen that, the emission of the  ${}^5\text{D}_0 \rightarrow {}^7\text{F}_2$  transition of  $\text{Eu}^{3+}$  decays exponentially, which can be well-fitted into the following exponential function:

$$I(t) = I_0 \exp(-t/\tau) + C$$

where  $I(t)$  and  $I_0$  is the luminescence intensity at time  $t$  and initial time,  $C$  is a constant which relates to the test equipment,  $t$  is the time and  $\tau$  is the decay lifetime for the exponential components, respectively. The measurement results of the luminescence lifetime

of the as-synthesized  $Y_{0.95}(P_{0.5}, V_{0.5})O_4:0.05Eu^{3+}$ ,  $(Y_{0.5}, Gd_{0.5})_{0.95}(P_{0.5}, V_{0.5})O_4:0.05Eu^{3+}$  and  $(Y_{0.5}, Gd_{0.5})_{0.9}(P_{0.5}, V_{0.5})O_4:0.05Eu^{3+}, 0.05Bi^{3+}$  samples at 619 nm emission under 275 nm excitation are 862.59, 805.12 and 525.38  $\mu s$ , respectively. Due to the excitation energy transfer occurs in a very short time in comparison with the relatively long fluorescence decay time, the nature of non-exponential decay cannot be attributed to the excitation energy transfer [25]. It can be noticed that with the doping of  $Bi^{3+}$ , the luminescence lifetime of  $(Y_{0.5}, Gd_{0.5})_{0.9}(P_{0.5}, V_{0.5})O_4:0.05Eu^{3+}, 0.05Bi^{3+}$  upon 275 nm decreased a lot. This phenomenon indicates that  $Bi^{3+}$  can involve the energy transfer rate among  $Eu^{3+}$  and other ions, correlated to the decay lifetime. Therefore, further researches on the formation of the energy transfer after the introduction of  $Bi^{3+}$  and other ions into  $Y(P, V)O_4:Eu^{3+}$  become very important.

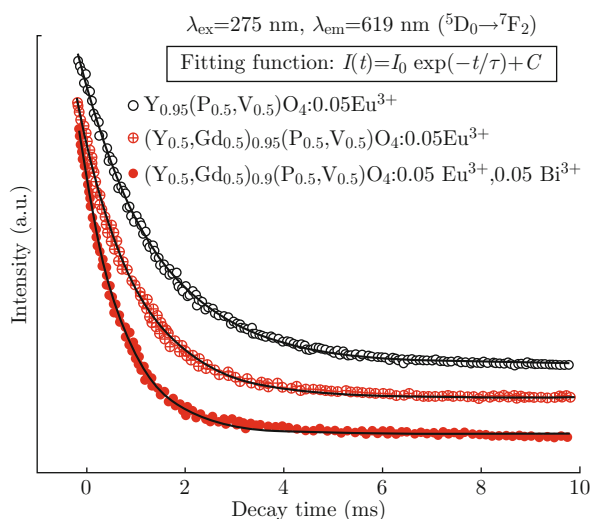


Fig. 6 The luminescence decay curves collected for  $Eu^{3+}$  emission ( ${}^5D_0 \rightarrow {}^7F_2$ ) under 275 nm excitation for  $Y_{0.95}(P_{0.5}, V_{0.5})O_4: 0.05Eu^{3+}$ ,  $(Y_{0.5}, Gd_{0.5})_{0.95}(P_{0.5}, V_{0.5})O_4: 0.05Eu^{3+}$  and  $(Y_{0.5}, Gd_{0.5})_{0.9}(P_{0.5}, V_{0.5})O_4: 0.05Eu^{3+}, 0.05Bi^{3+}$  samples prepared by the subsection method.

## Conclusions

In this paper, series of  $(Y_{1-y}, Gd_y)_{0.95-x}(P_y, V_{1-y})O_4:0.05Eu^{3+}, xBi^{3+}$  samples have been synthesized successfully through a subsection method. When doping concentration were  $x = 0.05, y = 0.5$ , the samples showed pure phase and present rod-like morphology. The morphology and size of the samples could be controlled by adjusting the ratios between the seeds and the doping ions. The average sizes for the phosphor particles were 100-150 nm length and 50-100 nm width. With the doping of  $Bi^{3+}, P^{5+}$  and  $Gd^{3+}$  ions, the samples showed high red emission at 619 nm ( ${}^5D_0 \rightarrow {}^7F_2$ ),

superior color saturation and broad excitation band (210-400 nm). The doping of  $Bi^{3+}$  and  $Gd^{3+}$  can increase the emission intensity at 619 nm under 365 nm excitation, and  $Bi^{3+}$  could decrease the fluorescent lifetime. The advantages may expand the application of the samples.

## Acknowledgements

The authors would like to thank Chongqing Key Laboratory of Micro/Nano Materials Engineering and Technology. This work was supported by the Program for New Material Development & Application innovative Research Team of Higher Education in Chongqing of China (Grant No. 201042).

## References

- [1] K. N. Shinde, S. J. Dhoble and K. Park, "Effect of synthesis method on photoluminescence properties of  $Na_2Sr_2Al_2PO_4Cl_9:Ce^{3+}$  nanophosphor", Nano-Micro Lett. 4(2), 78-82 (2012). <http://dx.doi.org/10.3786/nml.v4i2.p78-82>
- [2] W. S. Song, K. H. Lee, Y. S. Kim and H. Yang, "Tuning of size and luminescence of red  $Y(V,P)O_4:Eu$  nanophosphors for their application to transparent panels of plasma display", Mater. Chem. Phys. 135(1), 51-57 (2012). <http://dx.doi.org/10.1016/j.matchemphys.2012.04.013>
- [3] S. H. Dai, Y. F. Liu, Y. N. Lu and H. H. Min, "Microwave solvothermal synthesis of  $Eu^{3+}$ -doped  $(Y, Gd)_2O_3$  microspheres", Powder Technol. 202(1-3), 178-184 (2010). <http://dx.doi.org/10.1016/j.powtec.2010.04.036>
- [4] B. K. Grandhe, V. R. Bandi, K. Jang, S. Ramaprabhu, H. S. Lee, D. S. Shin, S. S. Yi and J. H. Jeong, "Multi wall carbon nanotubes assisted synthesis of  $YVO_4:Eu^{3+}$  nanocomposites for display device applications", Compos. Part B 43(1), 1192-1195 (2012). <http://dx.doi.org/10.1016/j.compositesb.2011.08.011>
- [5] C. Jang, S. M. Lee and K. C. Choi, "Optical characteristics of  $YVO_4:Eu^{3+}$  phosphor in close proximity to Ag nanofilm: emitting layer for mirror-type displays", Opt. Express 20(3), 2143-2148 (2012). <http://dx.doi.org/10.1364/OE.20.002143>
- [6] Y. S. Chang, Z. R. Shi, Y. Y. Tsai, S. Wuc and H. L. Chen, "The effect of  $Eu^{3+}$ -activated  $InVO_4$  phosphors prepared by sol-gel method", Opt. Mater. 33(3), 375-380 (2011). <http://dx.doi.org/10.1016/j.optmat.2010.09.018>
- [7] N. Ogorodnikov, V. A. Pustovarov, V. M. Puzikov, V. I. Salo and A. P. Voronov, "A luminescence and absorption spectroscopy study of  $KH_2PO_4$  crystals doped with  $Ti^{3+}$  ions", Opt. Mater. 34(9), 1522-1528 (2012). <http://dx.doi.org/10.1016/j.optmat.2012.03.018>
- [8] C. Mu and J. H. He, "Synthesis and luminescence properties of  $Eu^{3+}$  doped porous  $YVO_4$  nanowires by

- chemical precipitation in nanochannels”, *Mater. Res. Bull.* 47(2), 491-496 (2012). <http://dx.doi.org/10.1016/j.materresbull.2011.06.008>
- [9] X. Z. Xiao, G. Z. Lu, S. D. Shen, D. S. Mao, Y. Guo and Y. Q. Wang, “Synthesis and luminescence properties of  $\text{YVO}_4:\text{Eu}^{3+}$  cobblestone-like microcrystalline phosphors obtained from the mixed solvent-thermal method”, *Mater. Sci. Eng., B* 176(1), 72-78 (2011). <http://dx.doi.org/10.1016/j.mseb.2010.09.005>
- [10] J. H. Li, J. Liu and X. B. Yu, “Synthesis and luminescence properties of  $\text{Bi}^{3+}$ -doped  $\text{YVO}_4$  phosphors”, *J. Alloys Compd.* 509(41), 9897-9900 (2011). <http://dx.doi.org/10.1016/j.jallcom.2011.07.079>
- [11] L. P. Xie, H. W. Song, Y. Wang, W. Xu, X. Bai and B. Dong, “Influence of concentration effect and Au coating on photoluminescence properties of  $\text{YVO}_4:\text{Eu}^{3+}$  nanoparticle colloids”, *J. Phys. Chem. C* 114(21), 9975-9980 (2010). <http://dx.doi.org/10.1021/jp100828t>
- [12] D. Hreniak, J. Doskocz, P. Gluchowski, R. Lisiecki, W. Strek, N. Vu, D. X. Loc, T. K. Anh, M. Bettinelli and A. Speghini, “Enhancement of luminescence properties of  $\text{Eu}^{3+}:\text{YVO}_4$  in polymeric nanocomposites upon UV excitation”, *J. Lumin.* 131(3), 473-476 (2011). <http://dx.doi.org/10.1016/j.jlumin.2010.10.028>
- [13] S. H. Choi, Y. M. Moon and H. K. Jung, “Luminescent properties of PEG-added nanocrystalline  $\text{YVO}_4:\text{Eu}^{3+}$  phosphor prepared by a hydrothermal method”, *J. Lumin.* 130(4), 549-553 (2010). <http://dx.doi.org/10.1016/j.jlumin.2009.10.029>
- [14] D. S. Jo, Y. Y. Luo, K. Senthil, T. Masaki and D. H. Yoon, “Synthesis of high efficient nanosized  $\text{Y}(\text{V},\text{P})\text{O}_4:\text{Eu}^{3+}$  red phosphors by a new technique”, *Opt. Mater.* 33(8), 1190-1194 (2011). <http://dx.doi.org/10.1016/j.optmat.2011.02.007>
- [15] Q. Z. Dong, Y. H. Wang, L. L. Peng, H. J. Zhang and B. T. Liu, “Controllable morphology and high photoluminescence of  $(\text{Y}, \text{Gd})(\text{V},\text{P})\text{O}_4:\text{Eu}^{3+}$  nanophosphors synthesized by two-step reactions”, *Nanotechnol.* 22(21), 215604-215611 (2011). <http://dx.doi.org/10.1088/0957-4484/22/21/215604>
- [16] J. Wang, M. Hojamberdiev and Y. H. Xu, “CTAB-assisted hydrothermal synthesis of  $\text{YVO}_4:\text{Eu}^{3+}$  powders in a wide pH range”, *Solid State Sci.* 14(1), 191-196 (2012). <http://dx.doi.org/10.1016/j.solidstatesciences.2011.10.019>
- [17] K. Park and S. W. Nam, “VUV photoluminescence characteristics of  $(\text{Y}, \text{Gd})\text{VO}_4:\text{Eu}, \text{Zn}$  phosphors produced by ultrasonic spray pyrolysis”, *Mater. Chem. Phys.* 123(2-3), 601-605 (2010). <http://dx.doi.org/10.1016/j.matchemphys.2010.05.021>
- [18] S. Takeshita, T. Watanabe, T. Isobe, T. Sawayama and S. Niikura, “Improvement of the photostability for  $\text{YVO}_4:\text{Bi}^{3+}, \text{Eu}^{3+}$  nanoparticles synthesized by the citrate route”, *Opt. Mater.* 33(3), 323-326 (2011). <http://dx.doi.org/10.1016/j.optmat.2010.09.006>
- [19] J. Y. Sun, J. B. Xian, Z. G. Xia and H. Y. Du, “Synthesis, structure and luminescence properties of  $\text{Y}(\text{V},\text{P})\text{O}_4:\text{Eu}^{3+}, \text{Bi}^{3+}$  phosphors”, *J. Lumin.* 130(10), 1818-1824 (2010). <http://dx.doi.org/10.1016/j.jlumin.2010.04.016>
- [20] Y. Y. Zuo, W. J. Ling and Y. H. Wang, “Synthesis and photoluminescence properties of  $\text{YVO}_4:\text{Eu}^{3+}, \text{Al}^{3+}$  phosphor”, *J. Lumin.* 132(1), 61-63 (2012). <http://dx.doi.org/10.1016/j.jlumin.2011.07.012>
- [21] J. H. Shin, S. W. Choi, S. H. Hong, S. J. Kwon, S. Y. Seo, H. S. Kim, Y. H. Song and D. H. Yoon, “Luminescent properties of  $\text{Y}(\text{P}, \text{V})\text{O}_4:\text{Eu}^{3+}$  phosphors prepared by combining liquid phase precursor method and planetary ball milling”, *J. Alloys Compd.* 509(11), 4331-4335 (2011). <http://dx.doi.org/10.1016/j.jallcom.2011.01.060>
- [22] Y. P. Fang, A. W. Xu, R. Q. Song, H. X. Zhang, L. P. You, J. C. Yu and H. Q. Liu, “Systematic synthesis and characterization of single-crystal lanthanide orthophosphate nanowires”, *J. Am. Chem. Soc.* 125(51), 16025-16034 (2003). <http://dx.doi.org/10.1021/ja037280d>
- [23] Y. C. Chen, Y. C. Wu, D. Y. Wang and T. M. Chen, “Controlled synthesis and luminescent properties of monodispersed PEI-modified  $\text{YVO}_4:\text{Bi}^{3+}, \text{Eu}^{3+}$  nanocrystals by a facile hydrothermal process”, *J. Mater. Chem.* 22(16), 7961-7969 (2012). <http://dx.doi.org/10.1039/C2JM30756A>
- [24] C. C. Wu, K. B. Chen, C. S. Lee, T. M. Chen and B. M. Cheng, “Synthesis and VUV photoluminescence characterization of  $(\text{Y}, \text{Gd})(\text{V}, \text{P})\text{O}_4:\text{Eu}^{3+}$  as a potential red-emitting PDP phosphor”, *Chem. Mater.* 19(13), 3278-3285 (2007). <http://dx.doi.org/10.1021/cm061042a>
- [25] B. V. Rao and S. Buddhudu, “Emission analysis of  $\text{RE}^{3+}$  ( $\text{Dy}^{3+}$  or  $\text{Tb}^{3+}$ ): $\text{Ca}_3\text{Ln}(\text{=Y}, \text{Gd})(\text{VO}_4)_3$  powder phosphors”, *Mater. Chem. Phys.* 111(1), 65-68 (2008). <http://dx.doi.org/10.1016/j.matchemphys.2008.03.013>